

Cite this: *Lab Chip*, 2012, **12**, 127

www.rsc.org/loc

PAPER

Platinum nanoparticle-facilitated reflective surfaces for non-contact temperature control in microfluidic devices for PCR amplification

Daniel C. Leslie,^{†a} Erkin Seker,^{‡a} Lindsay A. L. Bazydlo,^{§a} Briony C. Strachan^a and James P. Landers^{*abc}

Received 19th August 2011, Accepted 27th October 2011

DOI: 10.1039/c1lc20779b

The polymerase chain reaction (PCR) is critical for amplification of target sequences of DNA or RNA that have clinical, biological or forensic relevance. While extrinsic Fabry-Perot interferometry (EFPI) has been shown to be adequate for non-contact temperature sensing, the difficulty in defining a reflective surface that is semi-reflective, non-reactive for PCR compatibility and adherent for thermal bonding has limited its exploitation. Through the incorporation of a reflective surface fabricated using a thermally driven self-assembly of a platinum nanoparticle monolayer on the surface of the microfluidic chamber, an enhanced EFPI signal results, allowing for non-contact microfluidic temperature control instrumentation that uses infrared-mediated heating, convective forced-air cooling, and interferometric temperature sensing. The interferometer is originally calibrated with a miniature copper-constantan thermocouple in the PCR chamber resulting in temperature sensitivities of -22.0 to -32.8 nm \cdot $^{\circ}\text{C}^{-1}$, depending on the chamber depth. This universal calibration enables accurate temperature control in any device with arbitrary dimensions, thereby allowing versatility in various applications. Uniquely, this non-contact temperature control for PCR thermocycling is applied to the amplification of STR loci for human genetic profiling, where nine STR loci are successfully amplified for human identification using the EFPI-based non-contact thermocycling.

Introduction

Accurate temperature control is crucial for the efficient execution of a variety of biochemical and chemical reactions and assays. Polymerase chain reaction (PCR) is among the most important of these and requires the greatest temperature resolution for efficient enablement as a tool for genetic analysis, pathogen detection, DNA sequencing¹ and human identification (ID).² The latter application arena involves the PCR amplification of short tandem repeat (STR) sequences at select loci in the human genome; the collective profile from a size-based separation of the amplified products provides the basis for forensic human ID analysis.² This size-based separation portion of the analysis has been successfully miniaturized for human ID, requiring small sample volumes (less than 1 μL).^{3–5} Conventional thermal cycling

schemes use tens of microliters of costly PCR reagents, with larger volumes and block thermocyclers, thereby significantly increasing assay duration (2–4 h).

Miniaturization technology is ideal for application to biochemical assays challenged with reducing costly reagents and excessive analysis times. However, miniaturization comes with its own challenges, most notably the difficulty to control the temperature of microscale liquid volumes (on the order of pico- to nano-liters) within the confined space of microchip architecture. Efforts to date to miniaturize the PCR portion of forensic human ID analysis have focused on directly measuring the solution temperature during thermocycling.⁶ These types of sensors can increase the time and labour involved in fabricating and operating the microfluidic device. Numerous approaches have been brought to bear on controlling temperature without direct contact of the solution, some involving the addition of a molecular probe into the solution. Kim *et al.* demonstrated a non-contact thermocycling of nanoliter aqueous droplets in oil for detection of human eukaryotic ribosomal genes (18S rRNA) in human genomic DNA using an infrared laser diode and temperature-sensitive fluorescent dye (LDS 698).⁷ Mondal *et al.* used SYBR green I, a fluorescent, DNA-intercalating dye, to monitor the temperature *via* fluorescence spectroscopy.⁸ This technique required the addition of nonspecific “sensor” DNA to the reaction mix to ensure that the levels of fluorescence did not change as nucleotides were polymerized to form DNA. Aside from the significant noise associated with fluorescence-based

^aDepartment of Chemistry, University of Virginia, McCormick Road, P.O. Box 400319, Charlottesville, VA, 22904, USA. E-mail: landers@virginia.edu; Fax: +1 434 243 8852; Tel: +1 434 243 8658

^bDepartment of Mechanical and Aerospace Engineering, University of Virginia, Charlottesville, VA, 22904, USA

^cDepartment of Pathology, University of Virginia Health Science Center, Charlottesville, VA, 22908, USA

[†] Current Affiliation: Wyss Institute for Biologically Inspired Engineering, Harvard University; Boston, MA, 02115, USA.

[‡] Current Affiliation: Department of Electrical and Computer Engineering, University of California, Davis; Davis, CA, 95616 USA.

[§] Current Affiliation: Dept of Pathology, Immunology, and Laboratory Medicine, University of Florida; Gainesville, FL, USA.

temperature sensing (variation on the order of multiple degrees Celsius), addition of DNA to any clinical or forensic sample would be difficult to prove innocuous. Separate fluorescent dyes in solution (rather than intercalating dyes) have also been used as temperature indicators in microfluidic thermocycling, with a reported relative error of greater than 1 °C unless sample averaging over 2 s per measurement.^{9–11} In general, dyes are sensitive to quenching agents in the solution and changes in pH, and systems shown to date lack stringent temperature resolution (<1.0 °C). Additional approaches included Raman thermometry for correlating solution temperature to O–H stretching of water molecules are effective but limited to a relatively narrow temperature range (50 to 60 °C).¹² The temperature-dependent absorption of water at 1412 nm has been used to measure temperature in 0.5 mm-thick films of water with a near-infrared camera.¹³

The common obstacle to all microfluidic non-contact temperature sensing approaches has been the lack of sensitivity, preventing the demands of successful amplification guided by multiple primer sets in a single PCR. We have previously demonstrated two non-contact measurement methods that yielded a finer temperature resolution. One method employed infrared (IR) pyrometric non-contact temperature sensing of the microdevice surface that was in contact with the solution.¹⁴ While the system exhibited high temperature resolution, it required tedious pyrometer calibration for proper sensor operation, thereby, diminishing the versatility of the method. A solution to this for on-chip calibration was provided by ‘azeotropic calibration’, but required that additional microfluidic architecture be fabricated. The other method utilized extrinsic Fabry-Perot interferometry (EFPI) to directly probe the solution temperature.¹⁵ First demonstrated for microscalar distance measurement by Murphy *et al.*,¹⁶ EFPI measures the optical path length (OPL) between two parallel reflective surfaces, which is proportional to the temperature-dependent refractive index changes and the physical depth of the Fabry-Perot cavity. Critical to exploiting interferometry for accurate temperature measurement (based on optical path changes in a liquid medium) is the fabrication of an inert, reflective coating in the microfluidic feature where solution temperature is to be measured.¹⁵ Previously, the reflective surfaces were produced by sputtering gold and chemically depositing silver.¹⁵ Unfortunately, these approaches had drawbacks as the silver coating was not compatible with the high ionic strength and temperature of PCR thermocycling¹⁷ and the gold lost its reflectivity during thermal bonding.¹⁵ The degradation of silver coating into the PCR solution adversely affected the efficiency of Taq DNA polymerase, consequently making DNA amplification impossible.¹⁵ In addition, gold layers require a thin, ‘adhesion’ layer of titanium or chromium to adhere to the glass surface, requiring additional fabrication steps, and both metals have been shown to inhibit PCR efficiency.^{18,19} Platinum does not require a seed layer for adhesion and has been used as an electrode surface in PCR microdevices.²⁰ It is, therefore, a promising material as a reflective coating for interferometric temperature sensing.

Here, we present the first account of a completely non-contact interferometric temperature control system (sensing, heating and cooling) for direct temperature measurement of solution during the PCR process. We have mitigated the aforementioned

challenges by coating the cavity surfaces with a thin layer of platinum, which: (i) withstands high temperatures required for glass bonding; (ii) exhibits optimal optical attributes for EFPI-based non-contact high-resolution temperature measurement; and (iii) enables compatibility with PCR solution constituents. In the process of characterization, we discovered that the platinum layer underwent an interesting transition from a continuous thin film to supported nanoparticles when heated to the bonding temperature of borosilicate glass (650 °C). We also determined a way to passivate the platinum surface with silicate and a silane coating for biochemical reactions. This paper discusses the device development and characterization, as well as demonstrates the applicability of this technology to successful STR amplification for human genetic profiling.

Materials and methods

AmpF/STR® MiniFiler™ PCR Amplification Kits and AmpliTaq Gold® DNA polymerase, with Buffer II and MgCl₂ solutions were obtained from Applied Biosystems (Carlsbad, CA). Human genomic DNA was purified from blood sample from a single donor with a Qiagen DNA purification kit. Bovine serum albumin (BSA) and purified λ-phage DNA were obtained from USB Corporation (Cleveland, OH). Taq DNA polymerase and PCR reagents from Fisher Scientific (Waltham, MA) were used for λ-phage PCR amplification. Potassium silicate solution (KASIL 6), which consisted of 12.65% K₂O and 26.5% SiO₂, was obtained from PQ Corporation (Malvern, PA). Light mineral oil was obtained from Sigma Corporation (St. Louis, MO).

Microdevices were fabricated from borosilicate glass (Schott, Inc.; Elmsford, NY) through photolithography and wet chemical etching, as previously described.²¹ After hydrofluoric acid etching, the photoresist was dissolved, but the chrome layer was not yet removed in order to mask the unetched surface from platinum deposition. The 4 nm-thick platinum film was deposited onto etched devices and blank glass covers with a magnetron sputtering system (Kurt J. Lesker Co.) by DC-sputtering of 99.99% pure platinum targets at a gun power of 200 W and process pressure of 10 mTorr of argon. Platinum thickness was measured using the thickness monitor installed in the sputtering system, which was calibrated using multiple Pt thicknesses achieved by varying deposition time at identical deposition conditions (*i.e.*, glass substrate, sputtering gun power, argon flow rate, and process pressure). The final platinum thickness was validated with a Veeco NT1100 optical profilometer. The strength of platinum adhesion to glass was qualitatively assessed by cleaning the Pt-coated chips in sonicated acetone and drying under nitrogen. Gold films deposited without an adhesion layer onto identical glass slides peeled during similar sonication and drying steps. A secondary validation was the observation that the platinum films remained intact (*i.e.*, no visually detectable scratch marks on metal surface) during the assembly of the microfluidic devices, which involved slight abrasion of the platinum surface with the cover glass. Gold films without an adhesion layer tended to scratch and peel during this assembly procedure. Following platinum deposition, the chrome layer was removed with CR-7 Chromium etchant from (Cyantek). The glass layers were thermally bonded at 650 °C. The surface morphology of platinum-coated Borofloat® before and after

annealing at 550 °C was observed by scanning electron microscopy (SEM) with a Zeiss FESEM SUPRA 40 instrument with 10 keV acceleration and 8.5 mm working distance. In order to make the devices more PCR-compatible, the entire microfluidic network was filled with a silicate solution (one part KASIL 6 potassium silicate solution, 9 parts deionized water, and 10 parts 1.5 M HCl) and baked for 1 h at 115 °C.²² A white precipitate formed and was rinsed out with deionized water.

A FiberPro USB interferometer (Luna Innovations; Roanoke, VA) was used to monitor the optical path length of the microfluidic chamber. The non-contact heating and cooling system (Fig. 1) was controlled with an in-house written LabVIEW program in real-time from the EFPI temperature reading. EFPI temperature sensing was calibrated by holding the temperature at 55, 60, 65, 70 and 75 °C for 30 s each while measuring both Δ OPL and temperature *via* thermocouple. The sensitivity of the change in OPL with temperature was determined by linear least squares fit with the five points from each hold. Because the change in refractive index with temperature ($\partial n/\partial T$) is not a constant value over the range of temperatures used for PCR

thermocycling, the annealing temperature range (55–75 °C) was calibrated as a linear function. A second calibration was used to find the programmed temperature that corresponds to an actual temperature of 95 °C. The Δ OPL for each device was measured at 95 °C and a similar calibration curve was obtained. The Δ OPL for the 95 °C hold for an arbitrary OPL₀ was converted into a temperature to program into the LabVIEW control program (generally 98–101 °C). The ambient temperature was 24 °C. Any shift in temperature before the start of EFPI monitoring shifts the actual temperature of the isothermal holds. This error could be corrected by adjusting the intercept of the calibration curve. Because $\partial n/\partial T$ is smaller at room temperature than at 50–95 °C, the error introduced by a 1 °C difference at 24 °C will correspond to less than 0.5 °C in the PCR range.

After fabrication, microdevices were rinsed with acetone and dried at 90 °C for 30 min, before passivation with SigmaCote (Sigma-Aldrich), a silanizing reagent, and a second 90 °C bake for 30 min. Microdevices that had been previously used were heated to 500 °C for 2 h to remove any organic residue on the surface before undergoing the same treatment as a new microdevice. After surface treatment of microdevices, λ -phage PCR solutions were made up consisting of 10 mM Tris-HCl, 50 mM KCl, pH 8.3, 4 mM MgCl₂, 0.2 mM each dNTP, 0.4 μ M forward and reverse primers, 0.02 units/ μ L Taq polymerase, 0.24 mg/mL BSA, and 2 to 3 ng/ μ L of λ -phage DNA. The DNA concentration was changed slightly to maintain approximately 1 ng in the chamber volume. 5 μ L MiniFiler PCR solutions were made up consisting of 40% v/v “AmpFISTR® MiniFiler™ PCR Master Mix,” 20% v/v “AmpF/STR® MiniFiler™ Primer Set” solution, 0.5 units/ μ L AmpliTaq Gold® Taq polymerase, 0.24 mg/mL BSA, and 1.5 ng/ μ L of purified human genomic DNA. The sample was introduced into the PCR chamber, and the reservoirs were covered with light mineral oil to prevent evaporation. λ -phage samples were thermocycled with IR-mediated heating with the following procedure: 95 °C for 1 min; 30 cycles of 95 °C for 5 s and 68 °C for 10 s; 72 °C final extension for 30 s. MiniFiler® samples were thermocycled with IR-mediated heating with the following procedure: 95 °C for 10 min; 30 cycles of 95 °C for 2 s, 59 °C for 2 min and 68 °C for 60 s; 72 °C final extension for 5 min. Sample was collected from the PCR chamber with a pipette and diluted into 25 μ L of either deionized water (λ -phage) or highly deionized formamide (MiniFiler). The MiniFiler samples were sized with an Applied Biosystems ABI PRISM® 310 Genetic Analyzer (Carlsbad, CA) with 5-color detection and GeneScan software.

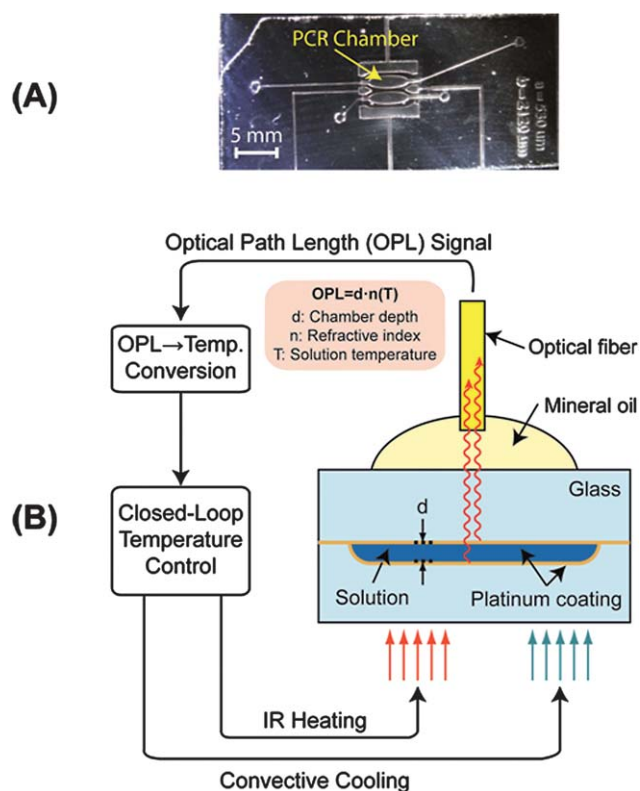


Fig. 1 EFPI monitoring of microfluidic chamber. A) Microfluidic device for non-contact PCR amplification. B) Broadband near-infrared radiation (850-nm max) is emitted through the optical fiber to the microfluidic chamber (50–200 μ m depth). This light is reflected by both thin, semi-reflective platinum layers on the top and bottom of the chamber. The reflected light is collected by the same fiber and the light from the two surfaces forms an interference pattern, which is used for extracting the optical path length between the two reflective surfaces. This OPL is dependent on the physical distance (d) between the reflective surfaces and the refractive index (n) of the medium in between. The refractive index decreases with increasing temperature (T), enabling the monitoring of temperature inside the chamber by tracking the change in OPL.

Results and discussion

Characterization of platinum coating

The interferometer requires light from both the top and bottom of the chamber to accurately determine the optical path length (OPL).^{15,16} This necessitates the chamber surface to be semi-transparent in order to allow transmission of light through the top surface onto the chamber floor, yet provide adequate reflectivity.¹⁵ Application of a thin (4 nm-thick) layer *via* sputtering addressed this by creating a partially-reflective glass surface and allowing glass-to-glass thermal bonding necessary for producing the final PCR microdevice. Passivation of the

platinum surface for biochemical reactions was achieved with a two part process of (1) coating with a silicate solution and (2) silanizing that coating with a lipid coating, rendering the surface hydrophobic. In order to quantify the effect of thermal exposure on optical properties of the coating, we annealed Pt-coated glass chips at the bonding temperature (550 °C). Prior to thermal annealing, the layer reflected or absorbed ~50% of the light across a wide range of the visible to near-infrared spectra (400 to 1100 nm wavelength light). Following annealing, the transmittance was generally higher, and the reflectivity gradually decreased with increasing wavelength (Fig. 2). The transmittance at the peak wavelength of the EFPI light source (850 nm) was still lower than uncoated borosilicate glass, suggesting an effective reflective coating (7.3% reflectivity) in the spectral region of interest.¹⁵ Preliminary testing showed a strong EFPI signal between two Pt-coated pieces of glass after thermal treatment (data not shown). The change in optical transmittance of the Pt-coated glass was accompanied by a distinct color change from dull metallic gray to a light brown providing a visual checkpoint for the formation of an effective reflective coating (Fig. 2). Further interrogation with scanning electron microscopy revealed the probable source of the color change to be the formation of nanometer-scale particles (10 to 100 nm in diameter) on the glass surface (Fig. 2, inset). Prior to the high temperature bake, the platinum layer appeared uniform and continuous across the glass surface. Afterwards, the glass was coated with a discontinuous layer of platinum islands, each only measuring tens of nanometers across. One possible explanation for the nanostructure formation may be that at the bonding temperature the platinum layer did not wet the glass surface uniformly and coalesced into small islands.^{23,24} The lower transmittance at the shorter wavelengths can also be explained by the presence of polydisperse platinum nano-islands on the glass

surface. Ultimately, the thin platinum coating maintained its reflectivity through the high temperature bonding process and allowed for thermal bonding of glass microdevices.

Validation of EFPI temperature monitoring

The change in OPL of the solution during thermocycling was compared to a reference temperature measurement to validate EFPI temperature monitoring in the microdevice. First, the OPL change in the PCR chamber was monitored *via* EFPI while the temperature of the platinum-coated microdevice was controlled by a miniature thermocouple inserted into the same chamber. The OPL changes closely coincided with thermocouple measurements (Fig. 3). The EFPI measurement was calibrated by correlating the change in optical path length (ΔOPL) values with thermocouple temperature values. The refractive index of water is dependent on solution temperature,²⁵ but the function is not linear over the range of interest for PCR amplification (50 to 95 °C). The magnitude of the change in refractive index with temperature ($\partial n/\partial T$) increases with temperature.²⁶ A smaller range (55 to 75 °C) was chosen to accommodate a linear calibration, where the greatest accuracy was required for specific annealing of primers. All eight calibration measurements of three different chamber depths had linear correlation coefficients greater than 0.99, suggesting linear calibration was adequate for temperature control during PCR. Whole PCR samples (including DNA and PCR solution) were used for calibrating the microdevice in order to account for all ionic effects on refractive index. The $\partial T/\partial\text{OPL}$ values obtained were consistent with, but slightly larger in magnitude than, those previously reported for pure water.²⁵ The linear correlation used for calibrating devices was $(\partial T/\partial\text{OPL}) = 0.1797(\text{OPL}_0) - 73.98$.

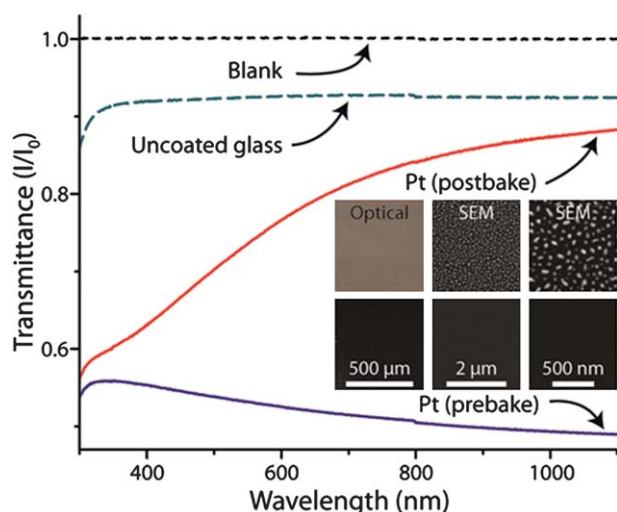


Fig. 2 Visible to near-infrared wavelength transmittance spectra for glass with and without platinum coatings. Borosilicate glass (green dashed line) sputtered with 4 nm of platinum (blue line) then baked at 550 °C (red line). Transmittance (black dashed line) is provided as reference. The inset illustrates the optical and scanning electron microscopy images of the platinum-coated glass surfaces before (top row) and after (bottom row) thermal treatment.

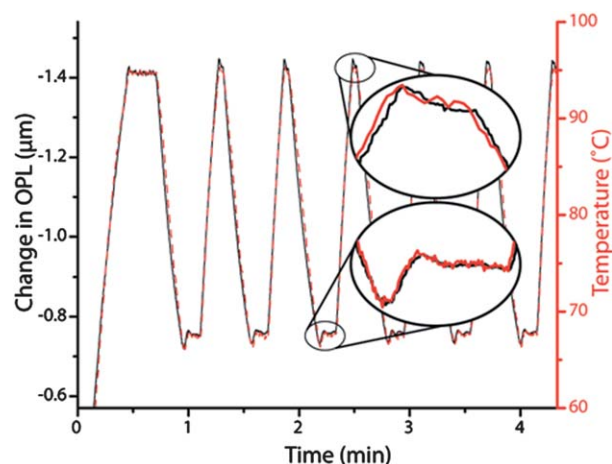


Fig. 3 Demonstration of the excellent agreement between the temperatures recorded *via* a thermocouple inserted into the microfluidic chamber (red dashes) overlaid with the change in optical path length (from initial OPL of 153 μm) acquired *via* the EFPI system from the same chamber (black line). The elliptical insets are close-up comparisons of the change in optical path length from the EFPI (black line) and the temperature measurement from the thermocouple (red line) in the microfluidic chamber first 68 °C hold (bottom) and second 95 °C hold (top).

The sensitivities of the EFPI-measured OPL with respect to temperature were -22.0 , -27.8 , and $-32.8 \text{ nm} \cdot ^\circ\text{C}^{-1}$ for OPL₀ values of 160, 208, and 242 μm , respectively, which resulted in a detectable temperature change of $0.3 \text{ }^\circ\text{C}$ for a thermocouple-based noise margin of $0.1 \text{ }^\circ\text{C}$. This suggests that the temperature resolution may be improved by using lower-noise thermocouples and higher quality signal acquisition circuitry. As this calibration is an intrinsic property of the solution, it is insensitive to changes in device architecture. Alternatively stated, in contrast to the approach using the IR pyrometer,¹⁴ this allows uncalibrated, virgin devices to be used to successfully amplify DNA, which is required for incorporation of 'single-use,' disposable microdevices in a bioanalytical instrument. The pyrometer-based non-contact thermocycling system also required a two-point calibration method for every new device based on boiling point determination of water and a 3-component azeotrope.¹⁵ With the demonstration of temperature sensing of PCR solution with high temperature resolution, completely non-contact PCR with IR-mediated heating, forced-air cooling, and EFPI-based temperature sensing could now be attempted.

EFPI-based non-contact PCR

In order to evaluate this non-contact thermocycling system, PCR of a 500-bp region of the λ -phage genome was chosen to provide evidence of temperature control and biochemical compatibility. Following the calibration, microdevices with various chamber depths were tested by first determining the initial OPL with PCR solution in the chamber. Then the specific calibration constant for that OPL₀ was determined using the equation for the linear fit of the calibration experiments. The non-contact system was first tested by amplifying a 500-bp region of λ -phage DNA in both chambers of microdevice, while a single chamber was monitored *via* EFPI. The electropherograms showed a strong peak in both chambers at the same size as the that associated with

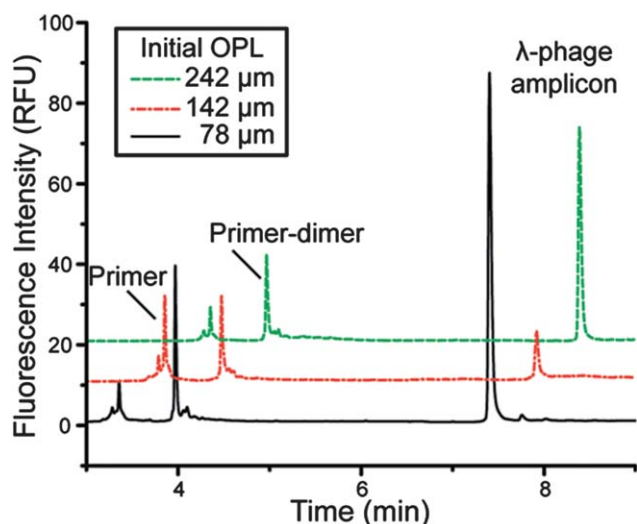


Fig. 4 Electropherograms of EFPI-PCR in chambers of different initial optical path lengths (roughly 4/3 of actual depth) demonstrating successful λ -phage amplification. The smallest chamber is too small to fit a miniature thermocouple in the chamber, revealing the calibration equation works below the lowest measured OPL₀.

conventional thermocycling in a polypropylene tube (data not shown), indicating that the device surface was sufficiently inert for biochemical analysis even through the rigors of high ionic strength and temperatures required for PCR. This demonstrates a significant improvement from the silver and gold coatings previously developed for EFPI temperature control for enzymatic reactions, which failed in amplifying DNA *via* PCR.¹⁵

The calibration was tested to determine the range of OPL₀ values where it was valid for PCR amplification. Microdevices with chamber depths within the calibration range (OPL₀ values of 142 and 242 μm) and below the established calibration range (OPL₀ value of 78 μm) were thermocycled *via* EFPI-based non-contact temperature sensing. All three devices successfully amplified the expected product, including the 78- μm -OPL₀ device (Fig. 4). It is important to note that this depth is too small to accommodate a miniature thermocouple (100 μm in diameter) for temperature sensing. This demonstrates the robust nature of the calibration. As the calibration is an intrinsic property of the solution, it should be applicable to most PCR samples, as they

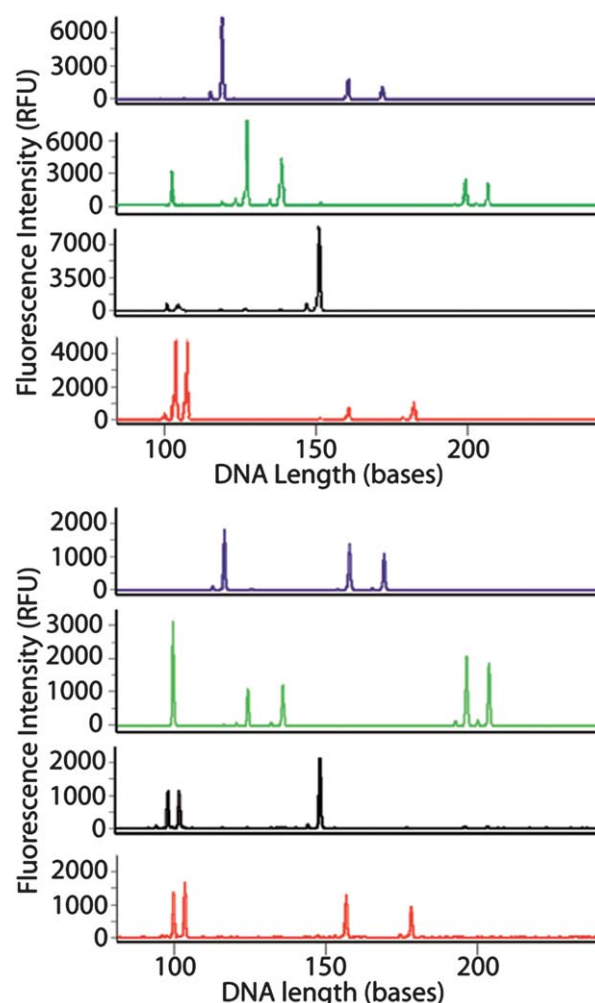


Fig. 5 Multicolor electropherograms of AmpF/STR® MiniFiler™ PCR amplification of human genomic DNA in the microfluidic device (1 μL reaction volume and 1 ng template DNA) using the EFPI-based non-contact temperature monitoring (top) and in a polypropylene tube using a conventional heating block thermocycler (bottom).

generally contain similar chemical components. Acknowledging that PCR is not quantitative, the differences in peak height between samples may be due to a variety of factors (insufficient collection of sample, differences in PCR efficiency, electrokinetic bias in electrophoretic analysis, *etc.*), but the migration time for all samples correlates with the λ -phage DNA 500-bp fragment indicative of successful PCR.

Non-contact human identification

As the final test, the system was challenged with a multiplex amplification (9 distinct primer pairs) to amplify 9 different loci of the human genome used in criminal cases for human identification based on forensic DNA analysis. Using a commercial kit where the components of the PCR master mix (concentration of primers, magnesium, buffer, *etc.*) have been formulated to amplify, with comparable efficiency, one or both allelic gene products from each of nine loci in the genome. This requires thermocycling that accurately reaches and holds the annealing temperature, with adequate dwell time at that temperature for all primer pairs to hybridize effectively with the complimentary sequences in the target DNA. The challenge associated with meeting the hybridization needs of multiple primer pairs, at least in this case, is highlighted by a 3.5 h total amplification time with conventional instrumentation. A genetic profile was obtained from human blood DNA amplified using the direct non-contact temperature sensing system completed in 2.5 h (Fig. 5, top). The genetic profile matched the profile obtained by conventional thermocycling in a polypropylene tube with a heating block (Fig. 5, bottom). This is the first reported multiplexed primer PCR amplification performed with non-contact thermocycling instrumentation.

Conclusions

A complete setup for non-contact PCR was demonstrated with successful amplification of a portion of λ -phage DNA and a commercially available amplification of human genomic DNA for human identification. The one-step platinum coating method enabled: (i) semi-reflective surfaces for non-contact high-resolution temperature measurements; (ii) non-reactive surfaces for PCR compatibility; and (iii) adherent surfaces for robust thermal bonding to produce microdevices. In addition, a calibration technique was developed that allowed for precise temperature control of microdevices with various chamber depths, including small dimensions that cannot be physically probed with miniature thermocouples. As the calibration depends on primarily the

intrinsic properties of an aqueous solution and not that of the device, we envision this method to be a universal temperature control scheme that can benefit a wide range of disposable miniaturized platforms, including cell-based devices, sequencing tools, and devices composed of different materials.

Acknowledgements

Daniel Leslie thanks the NIH for support under grant T32 GM08715.

Notes and references

- 1 M. A. Innis, D. H. Gelfand, J. J. Sninsky and T. J. White, *PCR protocols: a guide to methods and applications*, Academic Press, San Diego, CA, USA, 1990.
- 2 J. M. Butler, *Forensic DNA Typing: Biology and Technology behind STR Markers* Academic Press, San Diego, CA, USA, 2001.
- 3 J. M. Karlinsey and J. P. Landers, *Lab Chip*, 2008, **8**, 1285.
- 4 J. M. Karlinsey and J. P. Landers, *Anal. Chem.*, 2006, **78**, 5590–5596.
- 5 S. Yining, *Electrophoresis*, 2006, **27**, 3703–3711.
- 6 J. M. Bienvenue, L. A. Legendre, J. P. Ferrance and J. P. Landers, *Forensic Sci. Int.: Genet.*, 2010, **4**, 178–186.
- 7 H. Kim, S. Dixit, C. J. Green and G. W. Faris, *Opt. Express*, 2008, **17**, 218–227.
- 8 S. Mondal and V. Venkataraman, *J. Biochem. Biophys. Methods*, 2007, **70**, 773–777.
- 9 D. Ross, M. Gaitan and L. E. Locascio, *Anal. Chem.*, 2001, **73**, 4117–4123.
- 10 J. Coppeta and C. Rogers, *Exp. Fluids*, 1998, **25**, 1–15.
- 11 K. Sun, A. Yamaguchi, Y. Ishida, S. Matsuo and H. Misawa, *Sens. Actuators, B*, 2002, **84**, 283–289.
- 12 S. H. Kim, *et al.*, *J. Micromech. Microeng.*, 2006, **16**, 526.
- 13 N. Kakuta, K. Kondo, A. Ozaki, H. Arimoto and Y. Yamada, *Int. J. Heat Mass Transfer*, 2009, **52**, 4221–4228.
- 14 M. G. Roper, C. J. Easley, L. A. Legendre, J. A. C. Humphrey and J. P. Landers, *Anal. Chem.*, 2007, **79**, 1294–1300.
- 15 C. J. Easley, *et al.*, *Anal. Chem.*, 2005, **77**, 1038–1045.
- 16 K. A. Murphy, M. F. Gunther, A. M. Vengsarkar and R. O. Claus, *Opt. Lett.*, 1991, **16**, 273–275.
- 17 C. J. Easley, *Development and application of microfluidic genetic analysis systems*, Ph.D. Thesis, University of Virginia, 2006.
- 18 N. J. Panaro, X. J. Lou, P. Fortina, L. J. Kricka and P. Wilding, *Biomed. Microdevices*, 2004, **6**, 75–80.
- 19 T. B. Taylor, *et al.*, *Biomed. Microdevices*, 1998, **1**, 65–70.
- 20 T. H. Fang, *et al.*, *Biosens. Bioelectron.*, 2009, **24**, 2131–2136.
- 21 C. J. Easley, *et al.*, *Proc. Natl. Acad. Sci. U. S. A.*, 2006, **103**, 19272–19277.
- 22 L. A. Legendre, *Advancements in totally integrated microdevices for clinical diagnostics*, Ph.D. Thesis, University of Virginia, 2007.
- 23 G. L. Selman, M. R. Spender and A. S. Darling, *Platinum Met. Rev.*, 1965, **9**, 92–99.
- 24 E. Seker, *et al.*, *Acta Mater.*, 2007, **55**, 4593–4602.
- 25 R. C. Weast, W. H. Beyer (ed.), *CRC Handbook of Chemistry and Physics*, Vol. 69. CRC Press, Inc., Boca Raton, FL, 1988–1989.
- 26 G. Abbate, *et al.*, *J. Phys. D: Appl. Phys.*, 1978, **11**, 1167.